Single crystal structure refinement of tetramethylammonium-hectorite

Wolfgang Seidl and Josef Breu*

Universität Bayreuth, Lehrstuhl für Anorganische Chemie I, Universität Bayreuth, D-95440 Bayreuth, Germany

Dedicated to Professor Dr. Hans-Jörg Deiseroth on the occasion of his 60th birthday

Received July 22, 2004; accepted September 28, 2004

Pillared clays / Intercalation compounds / Hectorite / Tetramethylammonium / Single crystal structure analysis / X-ray diffraction

Abstract. A synthetic Cs-fluorohectorite was intercalated with Tetramethylammonium-cations (TMA^+). Under appropriate reaction conditions, a complete cation exchange is feasible while preserving the phase relationship between adjacent silicate layers. Starting from a three-dimensionally (3D) ordered [1] and homogeneously charged [2], synthetic Cs-hectorite it is possible to synthesize single crystals of a 3D ordered intercalation compound (TMA-hectorite). Single crystal structure refinement ($TMA_{0.5}{}^{inter}Mg_{2.5}Li_{0.5}{}^{oct}Si_4{}^{tet}O_{10}F_2$, monoclinic, $C2/m$, $a = 5.2735(11)$ Å, $b = 9.1165(14)$ Å, $c = 13.5609(35)$ Å, $\beta = 97.693(3)°$, $V = 646.1(2)$ Å^3, $Z = 2$) conclusively reveals the arrangement of the TMA-cations in the interlayer space. The results are compared with an earlier structure refinement of an analogous TMA-intercalated natural vermiculite [3] and the results of a computer simulation carried out on TMA-vermiculite [4].

Introduction

The intercalation of large molecular pillars into layered compounds opens up a universal route for the synthesis of porous materials. The most frequently used materials for this purpose are natural, swellable 2:1 layered silicates like smecites or vermiculites (Fig. 1). Additional functionality like chirality or catalytic properties can be introduced into the interlayer space by variation of the pillars. For instance, the replacement of inorganic cations by organic cations via ion exchange converts the clay surfaces from hydrophilic (due to strong hydration of inorganic cations) to hydrophobic. As a result, organoclays like the title compound, are highly effective sorbents for neutral organic contaminants and can be utilized in pollution prevention [5]. Despite the wide range of accessible physicochemical properties and promising applications (catalysis, nanotechnology, adsorbents, sensors and photo-functional materials [6–13]) there is little information available on the structure of these intercalation compounds. This stems mainly from two features inherent to natural clays:

1. Natural smectites and their intercalation compounds display no long range 3D order, which hampers the characterization by X-ray diffraction considerably. The structures are turbostratically disordered, i.e. adjacent silicate layers are shifted and/or rotated against each other by arbitrary values along the stacking direction. Therefore, beside 00*l*-reflections, the diffraction patterns contain only few broad *hk*-bands that result from diffraction of the two-dimensionally (2D) ordered silicate layers. Usually it is not possible to remedy the turbostratic disorder during an intercalation reaction [2]. However, cation exchange can be carried out even with large pillars leading to a considerable expansion of the interlayer space while preserving the phase relationship between adjacent silicate layers [3, 14–15]. A detailed discussion of the reasons why turbostratic disorder

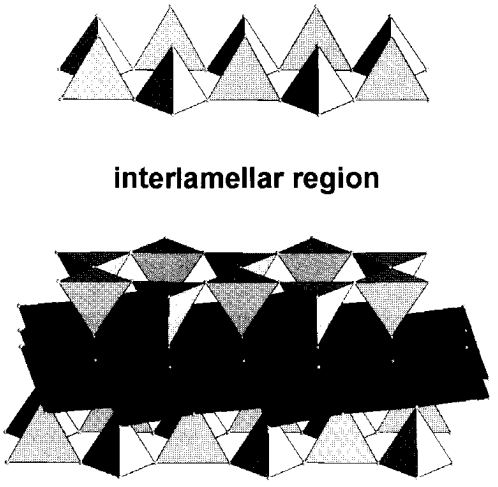

Fig. 1. Schematic illustration of the crystal structure of trioctahedral 2:1 phyllosilicates. Please note that in Fig. 3–5 only the two tetrahedral layers comprising the interlamellar region are shown.

* Correspondence author (e-mail: Josef.Breu@uni-bayreuth.de)

occurs and its effects on X-ray diffraction patterns can be found in [1, 15–16].

2. Another problem of natural layered silicates is, that the occurring isomorphic substitutions are not homogeneously distributed. This inevitably leads to inhomogeneities in layer charge regarding not only different silicate layers within a crystal but also different domains in a single silicate layer. Due to these inhomogeneities, a 2D long range order of the interlayer cations in a supercell can not be observed with natural smectites [2].

Despite the above problems, natural layered silicates are widely used because of their abundant availability and high intracrystalline reactivity that enables almost any intercalation reaction. However, the disadvantages of natural clays can be circumvented by using synthetic materials. Melt synthesis yields 3D ordered [1], homogeneously charged [2] Cs-fluorohectorites, which still show sufficient intracrystalline reactivity to produce 3D ordered intercalation compounds routinely [15]. In this paper the synthesis and single crystal structure refinement of TMA-hectorite is described and compared with an earlier structure refinement of an analogous TMA-vermiculite [3] and the results of computer simulations carried out on TMA-vermiculite [4].

Experimental

Intercalation reaction

The synthesis of the Cs-fluorohectorite was described in ref. [1] ($Cs_{0.5}{}^{inter}Mg_{2.5}Li_{0.5}{}^{oct}Si_4{}^{tet}O_{10}F_2$). Tetramethylammonium ($TMA^+$) was intercalated by boiling 300 mg of Cs-hectorite in 150 ml of a hydrous solution of 0.1 mol/l TMA-chloride for two days. This cation exchange was repeated 10 times with fresh exchange solutions.

The exchange progress was followed by powder XRD applying a STOE Stadi P equipped with a linear PSD detector (Stoe & Cie, Darmstadt, Cu$K_{\alpha 1}$, Ge-monochromator). See Fig. 2b for an intermediate stage of exchange. To remove the last traces of Cs^+, the concentration of the exchange solution was increased to 1 mol/l TMA-chloride in four final exchange steps. Also, 20 mg kryptofix [222] were added to slightly rise the selectivity for Cs^+ in the exchange solution. After this treatment an energy dispersive X-ray analysis (EDX) indicated that the cation exchange was complete. To remove any possibly intersalated excess of organic cations the TMA-hectorite was then boiled in 200 ml water for one day, filtered, washed with water and finally dried in air.

Single crystal X-ray data collection and refinement

Weissenberg rotation photographs were used to select an appropriate single crystal. One out of about thirty examined crystals of TMA-hectorite showed sharp and intense reflections with no visible diffuse scattering indicating a high degree of stacking order. To remove trace amounts of water that might be included in free voids of the interlayer space the selected crystal was then dried in high vacuum

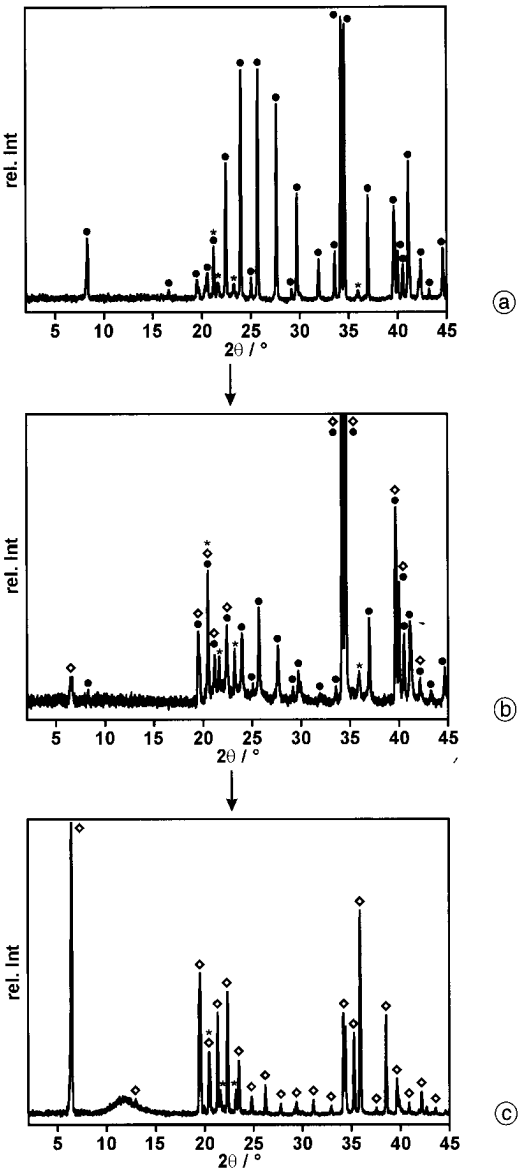

Fig. 2. Powder XRD-traces of Cs-hectorite (●) before (**a**), during (**b**) and after intercalation (**c**) to TMA-hectorite (◇). * = auxiliary tridymite.

for 4 days at 90 °C. After drying, the crystal was immersed in perfluorether to prevent rehydration from air.

To minimize dynamic disorder of the highly mobile interlayer cations, the data collection was carried out at 110 K. SHELX-97 [17] was used for data reduction, structure solution and refinement. Data were corrected for Lorentz and polarisation effects. The refinement itself was carried out on F^2 using all observed reflections. Further important details of the data collection are given in Table 1.

Structure solution using direct methods readily identified all atoms of the silicate host layer. However, as expected, the electron density in the interlayer space appeared highly diffuse. Therefore, the interlayer species (TMA-molecules) were treated as rigid bodies in the refinement. The starting coordinates of the interlayer cations in different orientations relatively to the silicate layer were generated with the help of the Cerius^2 [18] modelling software. Cerius^2 allows the interactive placement of TMA-

Table 1. Crystallographic data and additional information on data collection and structure refinement of TMA-hectorite.

Crystallographic data		
Formula unit		$TMA_{0.5}Mg_{2.5}Li_{0.5}Si_4O_{10}F_2$
Formular weigth		$M = 411.64$ g mol^{-1}
Crystal system		monoclinic
Space group		$C2/m$ (no. 12)
Lattice constants		$a = 5.274(1)$ Å
		$b = 9.117(1)$ Å
		$c = 13.561(4)$ Å
		$\beta = 97.69(3)°$
Volume of unit cell		646.1(2) Å^3
Z		2
D_x		2.281 g cm^{-3}
Radiation		MoK_α
Monochromator		graphite
Absorption coefficient		0.676 mm^{-1}
Temperature		110(1) K
Crystal colour and shape		colourless, hexagonal plate
Crystal dimensions		$0.20 \times 0.15 \times 0.03$ mm
Data collection		
Diffractometer		Stoe IPDS I
Reflections collected		3212
Unique reflections		831
R_{int}		0.0291
Unique reflections ($I_o > 2\sigma(I_o)$)		731
θ_{max}		28.78°
Index area		$h = -7 \rightarrow 7$
		$k = -11 \rightarrow 11$
		$l = -18 \rightarrow 18$
Absorption correction		none
Refinement		SHELX-97 [17]
$wR(F^2)$ (all data)		0.1018
$R(F)$ (observed) ($I_o > 2\sigma(I_o)$)		0.0372
$S(F^2)$ (all data)		1.088
Number of free parameters		68
$(\Delta/\sigma)_{max}$		0.000
Residual electron density	$\Delta\varrho_{max}$	1.276 e Å^{-3}
	$\Delta\varrho_{min}$	-0.678 e Å^{-3}

cations into the interlamellar region of the host lattice while controlling their orientation in a stereo view mode. The molecular structure of TMA^+ was taken from ref. [19]. The rigid body was maintained during the refinement with the help of the "FRAG" command in SHELXL-97. The symmetry of the parent compound ($C2/m$, SG. No. 12) was kept for the refinement. Clearly, only the host lattice rigorously adheres to this symmetry, while the electron density distribution in the interlayer space must possess a lower symmetry ($C1$ or lower). However, the interlayer space is sandwiched between two silicate surfaces that are stretched by the Kagome-net of basal oxygen atoms (compare Fig. 5). Thus the interlayer cations sense a very high hexagonal pseudo-symmetry which inevitably will lead to static disorder. This static disorder is approximated by applying the $C2/m$ symmetry also to the interlayer species. At this point, it should be noted that only about half of the interlayer positions are occupied. Therefore, the interlayer cations will tend to arrange in a 2D superlattice that is commensurable with the layer corrugation of the basal oxygen atoms. This 2D order in the interlayer space is reflected by a broad "bump" that became visible in the final powder diffraction pattern at approximately $12°/2\theta$ after the exchange reaction was complete (Fig. 2c). Due to the homogeneous layer charge of the host material, the pillars adopt a 2D "long range" order in each interlayer space. But this superstructure of interlayer cations can be arranged in several different energetically degenerated orientations with no correlation from one interlayer space to the adjacent ones. This will lead to a 2D band in the diffraction pattern. Furthermore, the large width of the superstructure band indicates that the ordering is far from perfect and/or the length scale of this 2D ordering of pillars is rather limited, meaning that the ordering only occurs in small domains. Here the atomic pair distribution function (PDF) analysis of powder diffraction data could prove very useful to investigate those small domains in detail, as it would reveal an average real distance of one pillar to its next neighbouring pillar.

For the structure refinement, this 2D band was neglected. The Bragg reflections used in the structure refinement contain only the averaged information on the in-plane arrangement and the orientation of interlayer cations relatively to the silicate layers. Nevertheless, from the Bragg diffraction valuable information can be deduced regarding the guest-guest and host-guest interactions in this intercalation compound.[1]

Results and discussion

Intercalation reaction

The progress of the intercalation reaction was carefully monitored by powder XRD. It should be stressed that intercalations are topotactic reactions which necessarily display only 2D cooperativity. In a first approximation, the intercalation in each interlayer space is independent from neighbouring interlayers. Due to this nature of the intercalation reaction in intermediate stages an interstratified material will be produced inevitably. Interstratification will in turn hamper the quality of data sets and therefore completeness of cation exchange must be carefully assured. This can be done by determining the variation coefficient (VC) and by checking for traces of unexchanged Cs^+ by EDX-analysis. The VC is a measure of the regularity of the stacking along the c-axis [16]. It is defined as the relative standard deviation of the mean value of basal spacings calculated from a series of $00l$-reflections. During a cation exchange reaction the two different basal spacings are

[1] Further information about the structure refinement can be requested from Fachinformationszentrum Karlsruhe, Gesellschaft für wissenschaftlich-technische Information mbH, D-76344 Eggenstein-Leopoldshafen 2, Germany, by indicating the deposition number CCDC-414249 (Email: crysdata@fiz-karlsruhe.de).

usually randomly distributed. In the powder diffraction pattern one then observes an averaged, "virtual" basal spacing which lies between the basal spacings of the adjacent end member reflections of the starting material and the intercalated compound. Moreover, for such a random interstratification, the 00*l*-reflections consequently are shifted in different directions in 2θ which increases the VC. Therefore, the VC is a very sensitive measurement to detect even small amounts of "wrong" basal spacings. From experience with our synthetic smectites, VCs of approximately 0.1% or less are exceptional good and can only be obtained after complete intercalation reactions. These values are much higher for natural or hydrothermally synthesized smectites. For instance, Capkova et al. observed a VC as high as 0.67 for a TMA-beidellite [20].

The starting material Cs-Hectorite (Fig. 2a) had a monoclinic unit cell with space group $C2/m$ (no. 12), $a = 5.2515(6)$ Å, $b = 9.0954(14)$ Å, $c = 10.8001(16)$ Å, $\beta = 99.281(9)°$, $V = 509.10(14)$ Å^3 and a very low VC of 0.03% (Table 4). During the initial stages of the intercalation reaction (Fig. 2b) two distinct sets of 00*l*-series are observed corresponding to Cs-hectorite and TMA-hectorite. This is because the kinetics of the intercalation reaction differ largly with the size and the aspect ratio of the crystals [15]. However, these two phases are no longer pure end members but represent interstratified materials. The "intermediate" TMA-hectorite shows a relatively large VC of 0.335% (Table 5) clearly indicating a still incompletely exchanged TMA-hectorite. After 14 exchange steps (Fig. 2c) a monoclinic unit cell with space group $C2/m$ (no. 12), $a = 5.2419(5)$ Å, $b = 9.0728(16)$ Å, $c = 13.665(3)$ Å, $\beta = 97.336(10)°$, $V = 644.6(3)$ Å^3 could be refined for the TMA-hectorite. A calculated VC of 0.05% (Table 6) and no traces of Cs^+ in the EDX-analysis proved a complete intercalation reaction.

Single crystal refinement of TMA-hectorite

In 1997 Vahedi-Faridi et al. published a structure model for a TMA-intercalate (**VF-G-model**) based on a single crystal structure refinement of a cation exchanged natural vermiculite [3] with a slightly higher layer charge of 0.85 as compared to the title compound. The cell parameters (determined at room temperature) of this TMA-vermiculite are similar to the TMA-hectorite (space group $C2/m$ (no. 12), $a = 5.353(1)$ Å, $b = 9.273(2)$ Å, $c = 13.616(6)$ Å, $\beta = 97.68(3)°$). The key features of this VF-G-model are:

1. the TMA-molecule is offset from the center of the interlayer region by 1.52 Å,
2. only one methyl group of the TMA-tetrahedron is keyed into the hexagonal cavity of the silicate layers,
3. the TMA-molecules are arranged with their C_3 axis perpendicular to the silicate layer bringing one face of the NC_4 tetrahedron parallel to the silicate layers.

One should note that Vahedi-Faridi et al. were not able to locate the complete interlayer cation due to the diffuse electron density in the interlamellar space, but only the N atom and the keying C atom. The final VF-G-model converged to $R(F)$ (observed) = 0.073 ($I_o > 6\sigma(I_o)$).

This VF-G-model has two major weak points:

1. Usually, 3D order of layered compounds is only observed when the interlamellar space is cross-linked by the interlayer species which assures well defined phase relationships between adjacent layers. This

Table 2. Atomic coordinates, site occupation factors and equivalent isotropic thermal displacement parameters (in Å^2) of TMA-hectorite.

Atom	Wyckoff position	Occ.	*x*	*y*	*z*	U_{equiv}
Si	8*j*	1	0.0981(1)	0.1668(1)	0.2960(1)	0.0089(2)
Mg1	4*h*	0.789(7)	1/2	0.1666(1)	1/2	0.0089(4)
Li1	4*h*	0.211	1/2	0.1666	1/2	0.0089
Mg2	2*d*	0.804(9)	0	0	1/2	0.0093(5)
Li2	2*d*	0.196	0	0	1/2	0.0093
F	4*i*	1	−0.3570(3)	0	0.4258(1)	0.0113(4)
O1	8*j*	1	0.1383(3)	0.1670(2)	0.4164(1)	0.0102(4)
O3	4*i*	1	0.0785(4)	0	0.2512(1)	0.0105(4)
O4	8*j*	1	−0.1645(3)	0.2523(2)	0.2509(1)	0.0106(3)
TMA (1)						
N1	8*j*	0.094(4)	1.390(3)	1.060(2)	1.001(1)	0.0338(19)
C1	8*j*	0.094(4)	1.473(6)	0.989(4)	0.910(3)	0.0338(19)
C2	8*j*	0.094(4)	1.445(5)	1.219(2)	1.000(3)	0.0338(19)
C3	8*j*	0.094(4)	1.108(4)	1.035(3)	1.000(2)	0.0338(19)
C4	8*j*	0.094(4)	1.532(5)	0.991(5)	1.093(2)	0.0338(19)
TMA (2)						
N2	8*j*	0.080(4)	1.474(6)	−1.080(2)	1.000(4)	0.0338(19)
C5	8*j*	0.080(4)	1.468(10)	−0.983(8)	0.911(7)	0.0338(19)
C6	8*j*	0.080(4)	1.676(5)	−1.193(4)	0.999(3)	0.0338(19)
C7	8*j*	0.080(4)	1.217(5)	−1.153(4)	0.998(3)	0.0338(19)
C8	8*j*	0.080(4)	1.527(8)	−0.989(8)	1.093(7)	0.0338(19)

Table 3. Selected interatomic distances in the host lattice and in the interlayer space (in Å) of TMA-hectorite.

Atoms		distance	Atoms		distance
Si–O	4(×)	1.618(2)–1.640(2)	Mg2–F	2(×)	2.013(2)
Mg1–F	2(×)	2.023(2)	Mg2–O	4(×)	2.088(2)
Mg1–O	4(×)	2.084(2)–2.084(2)			
TMA (1)			TMA (2)		
C1–O_{bas}	6(×)	3.32(2)–3.50(3)	C5–$O_{bas.}$	6(×)	3.30(2)–3.53(3)
C4–O_{bas}	6(×)	3.32(2)–3.45(3)	C8–$O_{bas.}$	6(×)	3.29(2)–3.47(3)
C3–O3	2(×)	3.43(3)–3.45(1)	C6–O4	2(×)	3.42(1)–3.45(2)
C2–O4	2(×)	3.53(4)–3.54(2)	C7–O4	2(×)	3.47(1)–3.51(2)

cross-linking has been observed in 3D ordered hectorites and their 3D ordered intercalation compounds [1, 14–15]. In the VF-G-model adjacent silicate layers are also arranged with their hexagonal cavities opposite of each other, but there is no conclusive reason apparent for this mutual arrangement since the interlayer cations in this model key only on one side of the interlamellar space into the silicate layers.

Table 4. Variation coefficient of the parent Cs-hectorite.

l	d(00*l*)	*l**d(00*l*)
1	10.665 Å	10.665 Å
2	5.328 Å	10.656 Å
3	3.553 Å	10.660 Å
4	2.665 Å	10.659 Å
5	2.132 Å	10.661 Å
	mean value	10.660 Å
	rms	0.003 Å
	VC	0.030%

Table 5. Variation coefficient of an "intermediate" TMA-hectorite (compare Fig. 2b).

l	d(00*l*)	*l**d(00*l*)
1	13.491 Å	13.491 Å
3	4.512 Å	13.535 Å
4	3.389 Å	13.555 Å
5	2.720 Å	13.600 Å
	mean value	13.545 Å
	rms	0.045 Å
	VC	0.335%

Table 6. Variation coefficient of TMA-hectorite.

l	d(00*l*)	*l**d(00*l*)
1	13.555 Å	13.555 Å
2	6.781 Å	13.562 Å
3	4.522 Å	13.565 Å
4	3.387 Å	13.547 Å
5	2.711 Å	13.557 Å
	mean value	13.557 Å
	rms	0.007 Å
	VC	0.050%

2. For clay intercalation compounds the electrostatic attraction between the positively charged interlayer species and the negatively charged silicate layers is by far the dominating interaction. This leads to a strong driving force that will always minimize the

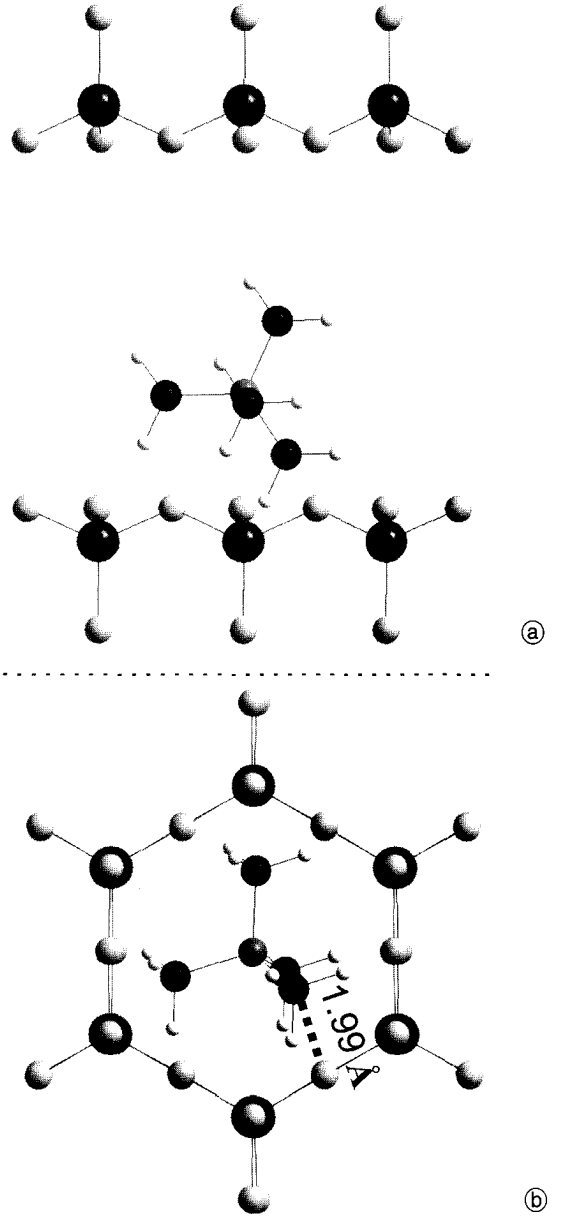

Fig. 3. Position and orientation of the TMA-molecules after refinement starting with the VF-G-model. View along *b* (**a**) and view along c^* (**b**). Atoms: H (white), C (black), N (medium grey), O (light grey), Si (dark grey).

interlayer distance [21]. Due to the large offset (1.52 Å) of the TMA-molecule from the center of the interlayer Vahedi-Faridi et al. identified a cavity of 1.7–2.4 Å between the base of the TMA-tetrahedron and the parallel basal oxygen atoms (labelled adsorption site B in Fig. 3 in ref. [3]). As pointed out above such a cavity is questionable because the system would be able to gain a lot of energy by reducing the basal spacing.

And indeed, Capkova et al. [4] were unable to confirm the VF-G-model by computer simulations. Static lattice energy minimisation proved that the structure suggested in the VF-G-model does not represent a local minimum. Starting with the VF-G-model the TMA-molecules reoriented during energy minimisation. The lattice energy minimum was observed with an orientation of the TMA-tetrahedron where one C–C edge points perpendicular to the silicate layers while the other C–C edge lies in the plane of the interlayer space (**C-model**, see Fig. 2 in ref. [4]). Moreover, the TMA-molecules are not shifted off the center but instead are arranged in one layer in the middle of the interlamellar region. The two methyl groups of the C–C edge that are oriented perpendicular to the silicate layers are keyed into the hexagonal hollows on both sides of the interlamellar region. They are not as deeply keyed into the cavities as suggested in the VF-G-model but, interestingly, they cross-link the silicate layers. In total, the C-model is physically more reasonable than the VF-G-model.

Interestingly, both models lead to a maximum of the interlayer electron density in the middle of the interlayer space, suggesting that the VF-G-model might have resulted by a structure refinement converging into a false minimum due to the diffuse electron density in the interlamellar space.

Therefore, we initially performed structure refinements starting with both these contradicting structure models.

VF-G-model refinement

Starting with the VF-G-model, the refinement converged to reliability factors of $R(F)$ (observed) = 0.0648 ($I_o > 2\sigma(I_o)$) and $wR(F^2)$ (all data) = 0.2064 and the residual electron density was in the range of +3.447 to −1.302 e/Å^3.

After refinement (Fig. 3) the pillars are still almost centered above a hexagonal cavity. The distances of the central N-atom of the TMA-molecule to the six basal oxygen atoms of the cavity vary from 3.34 to 3.41 Å. The organic interlayer cations are shifted by 1.26 Å from the middle of the interlayer space, considerably less than the 1.52 Å reported by Vahedi-Faridi et al. Moreover, forcing the refinement to take into account the electron density of the complete interlayer cation by applying a rigid body, led to a reorientation of the molecule. The C_3 axis of TMA^+ is no longer perpendicular to the silicate layers but tilted towards the *ab*-plane. Consequently, the apical methyl group is shifted away from the middle of the hexagonal cavity to one side. Short non-bonding distances occur between the face of the tetrahedral pillar and the basal oxygen atoms that vary from 1.99 to 2.80 Å. Considering the vdW-radii (O = 1.5 Å and C = 1.7 Å), it becomes obvious that these three methyl groups are too close to the hexagonal cavity (Fig. 3b). A very repulsive overlap of these methyl groups with basal oxygens atoms would result, which renders this pillar position and orientation doubtable.

C-model refinement

Starting with the C-model, the refinement quickly converged to considerably lower reliability factors as compared to the VF-G-model ($R(F)$ (observed) = 0.0464 ($I_o > 2\sigma(I_o)$) and $wR(F^2)$ (all data) = 0.1336), also the residual electron density improved significantly (+1.776 to −1.308 e/Å^3).

After the refinement (Fig. 4) the TMA-molecules are still positioned in the middle of the interlayer space, but they are not centered above a hexagonal cavity any more. The distances of the nitrogen atom to the basal oxygen atoms on both sides of the interlayer space vary from 3.82

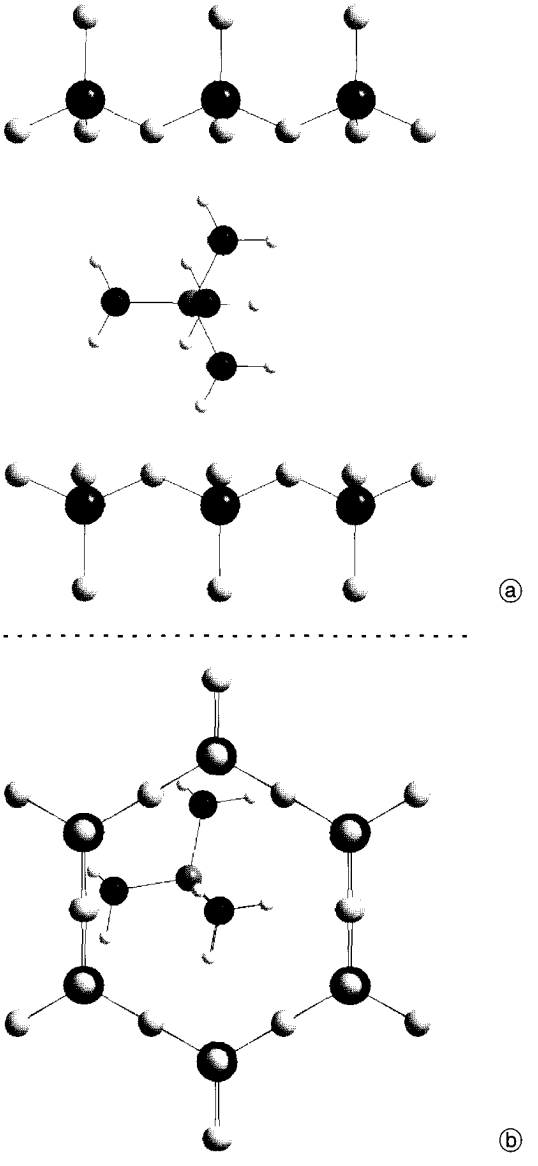

Fig. 4. Position and orientation of the TMA-molecules after refinement starting with the C-model. View along *b* (**a**) and view along c^* (**b**). Atoms: H (white), C (black), N (medium grey), O (light grey), Si (dark grey).

to 4.83 Å. Two of the methyl groups lie in the *ab*-plane, whereas the remaining two methyl groups point up and down. They key into the cavities of the two silicate layers and cross-link the interlamellar space. As the pillars are shifted from the center of the hexagonal cavity these two methyl groups are positioned exactly in the middle of the hexagonal cavities. When comparing the distances with vdW-radii (O = 1.5 Å and C = 1.7 Å) no overlap of pillar atoms and basal oxygen atoms is observed in the C-model. The distances between these two carbon atoms and the respective basal oxygen atoms of the adjacent silicate layers vary in a close range from 3.34(5) to 3.45(4) Å (Note that HO distances are meaningless since the torsion angles could not be refined with rigid bodies. Therefore, only distances between "heavy" atoms are cited.).

Altogether, the refined structure is very close to the starting C-model, the non-bonding distances are physically reasonable and the reliabliabilty factors are much lower than with the VF-G-refinement. Moreover, it is very reassuring that both refinements, against electron densities as measured by XRD, and against lattice energies converge to the same minimum.

Final refinement of TMA-hectorite

Comparing the refinements starting with the VF-G-model and the C-model it becomes obvious that the latter closer resembles the real electron density in the interlayer region. However, even when applying the symmetry operations of space group $C2/m$ to a single TMA-molecule in the interlayer, the high hexagonal pseudo symmetry that is sensed by the interlayer cation is inadequately matched and consequently the immanent static disorder is only poorly approximated. In reality, the pillars will be adopting several energetically degenerate orientations that all have the same host-guest arrangement. The mutual orientation of neighbouring guests, however, vary by rotation around the C–C edge that is perpendicular to the silicate layers. This statement is also strongly supported by the computer modelling results. Capkova et al. performed their lattice energy minimisations in a $2a2b$ supercell applying $P1$ symmetry giving all six cations surrounding a central cavity the freedom to rotate. In the minimized arrangement of TMA-cations in the interlayer space (see Fig. 3 in ref. [4]) indeed all neighbouring cations are mutually rotated. This suggests that the structure of the interlayer has a symmetry lower than $C1$. And the broad "bump" that became visible in the final powder diffraction pattern at approximately $12°/2\theta$ after cation exchange implies that the real unit cell even must be a supercell.

Unfortunately, refinement of the TMA-hectorite in a supercell or in $P1$ is not stable. Therefore, for the final refinement instead of lowering the symmetry, a second pillar was introduced into the interlayer space to better mimic the orientational disorder of interlayer cations. This second pillar orientation reduces the reliability factors again significantly ($R(F)$ (observed) = 0.0372 ($I_o > 2\sigma(I_o)$) and $wR(F^2)$ (all data) = 0.1018) and also, the residual electron density decreases (+1.276 to −0.678 e/Å^3).

In Fig. 5 the packing of the interlayer cations is displayed as space filling model. Figure 5a illustrates the

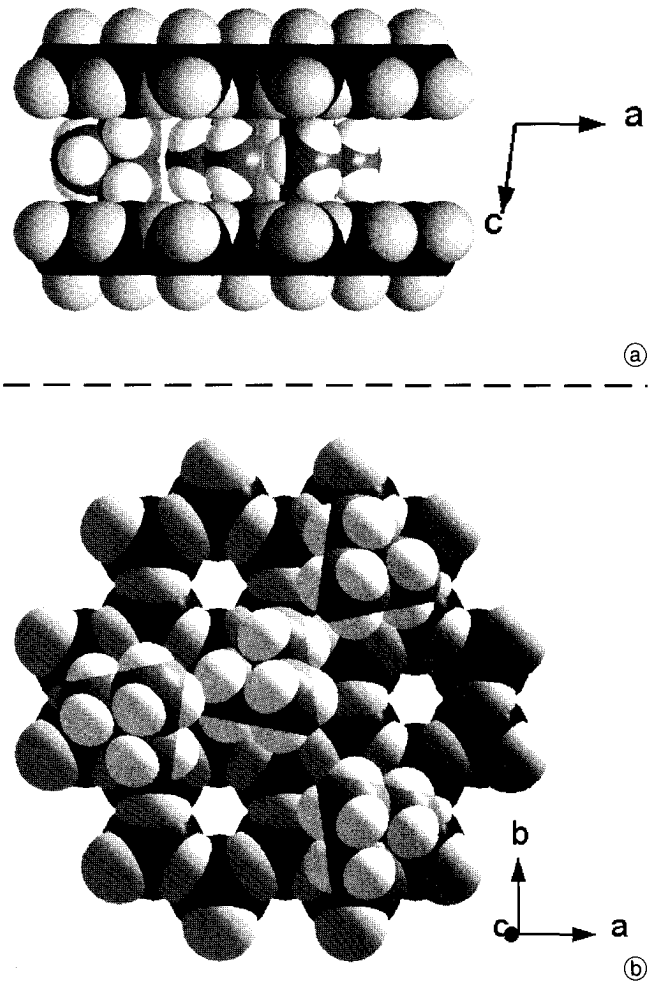

Fig. 5. Space filling model of the packing of pillar TMA (1) in the interlayer space viewed along b (**a**) and c^* (**b**). Atoms: H (white), C (medium grey), O (light grey), Si (dark grey). Note that only one of the symmetry related pillars per cavity is shown.

cross-linking nature of the C–C-edge that is perpendicular to the silicate layers. In Fig. 5b a realistic occupation of $^2/_3$ of interlayer positions is depicted. For the four interlayer cations shown, all short inter-pillar contacts are above the sum of vdW radii, the shortest contact is 3.4 Å. However, these reasonable intermolecular distances can only be realised by surrounding the central cation by TMA-molecules that are related by the 2-fold axis or the mirror plane. Similar to what has been observed in the lattice energy minimisation neighbouring molecules must be rotated in order to avoid unrealistically close contacts. Would the neighbouring molecules all have the same orientation, non-bonding contacts as close as 3.0 Å would result. This local disorder might also explain why the TMA-hectorite displays no sharp 2D superstructure bands as would be expected for a well developed 2D long range order of interlayer cations.

As has been observed for the parent Cs-hectorite, the occupation of the interlayer cation site (Table 2) is slightly higher than what would be expected from the bulk composition ($TMA_{0.696}$ instead of $TMA_{0.5}$). The structure of the host lattice is rigid and changes little upon intercalation (Table 3).

Conclusion

Even if the host lattice is 3D ordered and shows no rotational and/or translational stacking faults, structure refinement of the interlayer species remains difficult. Due to the nature of the intercalation reaction the electron density in the interlayer space inherently will be diffuse. The phase relationship between adjacent interlayers is not fixed because consecutive interlayers are far apart and the interaction is too weak. Therefore, even if a well ordered 2D structure is developed in the interlamellar region, different interlayers will be shifted and/or rotated relatively to each other.

Consequently, the Bragg reflections contain only the averaged information on the in-plane arrangement and the orientation of interlayer cations relatively to the silicate layers. Nevertheless, from the Bragg diffraction valuable information can be deduced regarding the guest-guest and host-guest interactions in intercalation compounds.

Identification (through difference fourier maps) and refinement of individual interlayer atoms, however, is risky and may easily lead into false minima. Refining interlayer cations as complete rigid bodies is therefore advantageous.

Following this strategy we were able to unequivocally decide between two contradicting structural models of TMA-vermiculites found in the literature.

As expected for a 3D ordered intercalation compound the interlayer cations key into the silicate layers on both sides and this way cross-link the interlamellar space.

Acknowledgment. We would like to thank the DFG for financial support.

References

[1] Breu, J.; Seidl, W.; Stoll, A. J.: Disorder in Smectites in Dependance of the Interlayer Cation. Z. Anorg. Allg. Chem. **629** (2003) 503–515.

[2] Breu, J.; Seidl, W.; Stoll, A. J.; Lange, K. G.; Probst, T. U.: Charge homogeneity in synthetic fluorohectorite. Chem. Mater. **13** (2001) 4213–4220.

[3] Vahedi-Faridi, A.; Guggenheim, S.: Crystal Structure of Tetramethylammonium-Exchanged Vermiculite. Clays Clay Miner. **45** (1997) 859–866.

[4] Capkova, P.; Burda, J. V.; Weiss, Z.; Schenk, H.: Modelling of Aniline-Vermiculite and Tetramethylammonium-Vermiculite; Test of Force Fields. J. Mol. Model. **5** (1999) 8–16.

[5] Chun, Y.; Sheng, G. Y.; Boyd, S. A.: Sorptive Characteristics of Tetraalkylammonium-exchanged Smectite Clays. Clays Clay Miner. **51** (2003) 415–420.

[6] Cheng, S.: From Layer Compounds to Catalytic Materials. Catal. Today **49** (1999) 303–312.

[7] Lerf, A.: Intercalation Compounds in Layered Host Lattices: Supramolecular Chemistry in Nanodimensions. Vol. 5: Organics, Polymers, and Biological Materials, pp. 1–166. Academic Press, San Diego, 2000.

[8] Mallouk, T. E.; Gavin, J. A.: Molecular Recognition in Lamellar Solids and Thin Films. Acc. Chem. Res. **31** (1998) 209–217.

[9] Ogawa, M.; Kuroda, K.: Photofunctions of Intercalation Compounds. Chem. Rev. **95** (1995) 399–438.

[10] Thomas, J. K.: Photophysical and Photochemical Processes on Clay Surfaces. Acc. Chem. Res. **21** (1988) 275–280.

[11] Thomas, J. M.: Uniform Heterogeneous Catalysts – the Role of Solid-State Chemistry in Their Development and Design. Angew. Chem. Int. Ed. **27** (1988) 1673–1691.

[12] Vaccari, A.: Clays and Catalysis: a Promising Future. Appl. Clay Sci. **14** (1999) 161–198.

[13] Varma, R. S.: Clay and Clay-supported Reagents in Organic Synthesis. Tetrahedron **58** (2002) 1235–1255.

[14] Slade, P. G.; Dean, C.; Schultz, P. K.; Self, P. G.: Crystal Structure of a Vermiculite Anilinium Intercalate. Clays Clay Miner. **35** (1987) 177–188.

[15] Breu, J.; Seidl, W.; Senker, J.: Synthesis of Threedimensionally Ordered Intercalation Compounds of Hectorite. Z. Anorg. Allg. Chem. **630** (2004) 80–90.

[16] Moore, D. M.; Reynolds, R. C.: X-Ray Diffraction and the Identification and Analysis of Clay Minerals. Oxford University Press, Oxford, 1997.

[17] Sheldrick, G. M.: SHELX-97, University of Göttingen, 1997.

[18] Molecular Simulation, Cerius, MSI, 9658 Scranton Road, San Diego, CA 92121-2777, USA, 1996, Ver. 2_3.5.

[19] Kornath, A.; Blecher, O.; Ludwig, R.: Preparation of Tetramethylammonium Azidosulfite and Tetramethylammonium Cyanate Sulfur Dioxide-adduct, $[(CH_3)_4N]^+[SO_2]N_3]^-$, $[(CH_3)_4N]^+ \cdot [SO_2OCN]^-$ and crystal structure of $[(CH_3)_4N]^+[SO_2]N_3]^-$. Z. Anorg. Allg. Chem. **628** (2002) 183–190.

[20] Capkova, P.; Pospisil, M.; Miehe-Brendle, J.; Trchova, M.; Weiss, Z.; le Dred, R.: Montmorillonite and Beidellite Intercalated with Tetramethylammonium Cations. J. Mol. Model. **6** (2000) 600–607.

[21] Breu, J.; Catlow, C. R. A.: Chiral Recognition among Tris(diimine)-metal Complexes. 4. Atomistic Computer Modeling of a Monolayer of $[Ru(bpy)_3]^{2+}$ Intercalated into a Smectite Clay. Inorg. Chem. **34** (1995) 4504–4510.